

Received April 16, 2021, accepted May 6, 2021, date of publication May 14, 2021, date of current version May 24, 2021.

Digital Object Identifier 10.1109/ACCESS.2021.3080317

Effect of Weather Condition on LoRa IoT Communication Technology in a Tropical Region: Malaysia

OLAKUNLE ELIJAH¹, (Member, IEEE),
SHARUL KAMAL ABDUL RAHIM¹, (Senior Member, IEEE),
VITAWAT SITTAKUL², AHMED M. AL-SAMMAN³, MICHAEL CHEFFENA³,
JAFRI BIN DIN¹, AND ABDUL RAHMAN THAREK¹

¹Wireless Communication Center, Faculty of Engineering, School of Electrical Engineering, Universiti Teknologi Malaysia, Johor Bahru 81310, Malaysia

²Department of Electrical Engineering Technology, College of Industrial Technology, King Mongkut's University of Technology North Bangkok, Bangkok 10800, Thailand

³Faculty of Engineering, Norwegian University of Science and Technology (NTNU), 2815 Gjøvik, Norway

Corresponding author: Vitawat Sittakul (vitawat.s@cit.kmutnb.ac.th)

This work was supported in part by the Kementerian Pengajian Tinggi (KPT), and in part by the Universiti Teknologi Malaysia under Grant 5F237, Grant 3F508, and Grant Q. J130000.21A2.05E25.

ABSTRACT An experimental study on the effect of weather conditions such as solar radiation, humidity, temperature, and rain on the Long Range (LoRa) communication in a tropical region (Malaysia) via a campus environment has been carried out and analyzed. The weather parameters were obtained from an online meteorological weather station (Meteoblue) and the use of a local automatic weather station. A temperature sensor was attached to the LoRa node to measure the onboard temperature. We analyze the diurnal variation and the effects of the weather condition based on the LoRa link in a LoRaWAN setup. A regular pattern of RSSI was observed with stronger RSSI values having a positive correlation with the atmospheric temperature, onboard temperature, and solar radiation during the day but degrades in late evenings. The positive correlation and pattern observed can be attributed to the prevailing meteorological conditions and opens room for further research needed for propagation modeling. The RSSI signals and relative humidity, on the other hand, showed no correlation. Furthermore, strong RSSI signals were obtained when the atmospheric temperature was between 30 - 40 °C, and the onboard temperature between 40 - 50 °C. No significant impact was observed on the RSSI signals when the rainfall rates vary from 12 mm/h to 180 mm/h. The study presents useful information to be considered on the effects of weather conditions in the propagation model and deployment of LoRa for IoT communication.

INDEX TERMS Humidity, internet of things (IoT), LoRa, LoRaWAN, RSSI, solar radiation, temperature, weather condition.

I. INTRODUCTION

LoRa communication technology is an unlicensed internet of things (IoT) technology that is characterized by low bandwidth, a limited number of messages, low power requirements, long-range communication, and higher penetration power [1]–[3]. The physical layer of the LoRa employs a chirp spread spectrum (CSS) modulation which enables long-range communication [4]. LoRa has been deployed for several IoT use cases such as smart city, agriculture, health,

water quality monitoring, tracking, and many other applications [5], [6]. While LoRa seems promising, studies have been conducted to investigate the impact of weather conditions such as temperature and humidity on the reliability of LoRa. For instance, laboratory experiments have been conducted to see the effects of temperature on the received signal strength indicator (RSSI) and signal-to-noise ratio (SNR) by radiating heat on the LoRa transceiver radio [7], [8]. While the studies in [7], [8] is limited to a controlled experiment using a TempLab testbed [9] to investigate the impact of onboard temperature on LoRa devices, [10]–[12] have provided insight on the effect of atmospheric temperature on

The associate editor coordinating the review of this manuscript and approving it for publication was Mohamed M. A. Moustafa¹.

the LoRa communication link. Extreme weather conditions were considered in northern Sweden [10] with average temperatures ranging from -16.96 to 13.22 °C [10] and Bosnia with temperatures of -5 to 4.5 °C [11]. While the results in [10], [11] indicated that atmospheric temperature can affect the RSSI and SNR of the LoRa, [12] shows that aside from temperature or humidity, LoRa link can be affected by some diurnal variation of the propagation caused by the changes in the troposphere. However, none of these works have shown or quantify the range of temperature in which LoRa performs well. In addition, some of these works on the effect of atmospheric temperature on the LoRa link were studied for a very short duration (two hours) [11] and in a very cold climate [10], [11]. Furthermore, during the deployment of the LoRa in our initial experiments, it was observed that packet loss was greater in the evenings and nights compared to during the day. This observation led to the investigation of the effect of weather parameters on the LoRa link.

To the best of our knowledge, studies on the impact of onboard, atmospheric temperature, and solar radiation on LoRa in the tropical region and the diurnal variation of the RSSI have not been reported. To bridge this gap, we investigate the effect of weather conditions on the LoRa link in a LoRaWAN set-up in a tropical region, Malaysia. The effects of onboard and atmospheric temperature and the impact of rain were considered. More importantly, we investigate the relationship of solar radiation on the RSSI LoRa link in a tropical region. The following contributions are provided: first, the study on the impact of solar radiation on the RSSI shows a positive correlation with the onboard and atmospheric temperature. This may be attributed to meteorological conditions prevalent at the time of the study. Secondly, the study shows that stronger RSSI is obtainable as the onboard and atmospheric temperature increase and even performs better within a certain temperature range. Thirdly, the study of the impact of rain shows that a high rainfall rate does not affect the LoRa link performance significantly, and fourthly, the study on the impact of relative humidity showed no correlation with the RSSI signal.

The rest of this paper is structured as follows. Section II presents the experimental set-up and Section III discusses the results and analysis. Section IV concludes this paper.

II. EXPERIMENTAL SET-UP FOR THE LoRaWAN

An outdoor gateway (GW) RHF2S008 was set up at the Wireless Communication Center (WCC), University of Teknologi Malaysia (UTM) Johor Bahru campus ($1^{\circ}33'30.8''N$ $103^{\circ}38'36.5''E$) and a LoRa test device was developed using the Pycom-Fipy with radio module Semtech SX1272 LoRa transceiver. The LoRa test device consists of GPS module, temperature sensor DS18B20 attached to the LoRa Radio and micro-controller board, buttons (connection, transmit, and reset buttons), and a menu that allows for configuration of different spreading factor (SF) and payload size. The GW was registered on the LORIIOT network server [13] using a free license. The LORIIOT network server which

was developed by the LORIIOT company for long-range IoT solution enables large-scale network deployment and is based on the LoRaWAN protocol and supports several types of GWs. It provides real-time access to LoRaWAN data using the WebSocket, hypertext transfer protocol (HTTP) push, transport layer security (TLS) socket, and message queuing telemetry transport (MQTT). The set-up of the experiment is shown in Fig. 1. The activation method used for the LoRa test device to join the LoRaWAN was over-the-air-activation (OTAA).

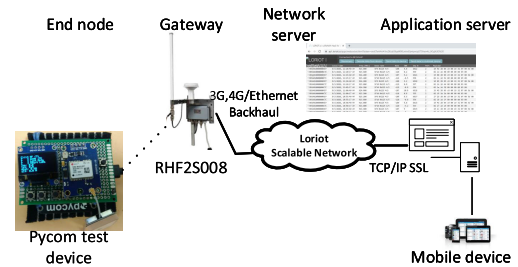


FIGURE 1. Experimental Set-up: LoRa test equipment, RHF2S008 GW, LORIIOT network server.

The geographical location of the GW and distance of the LoRa node from the GW are shown in Fig. 2. The GW and the LoRa node are located at an altitude of 40 m and 28 m above sea-level, respectively. The area is a large open space with an open field and lake surrounded by some buildings and light vegetation. The communication is non-line of sight (NLOS) due to the topology and some obstructions between the LoRa node and GW.



FIGURE 2. Location of the LoRa device and GW, University of Technology Malaysia, Johor Bahru.

The system configuration and parameters for the test conducted are summarized in Table 1. The atmospheric temperature and the amount of rainfall were measured using the Hobo rain gauge [14]. To observe the effect of the environmental conditions, the LoRa transmission frequency from the LoRa device to the GW was a 1-minute interval hence sampling time was 1-minute. The LoRaWAN operates a fairness policy

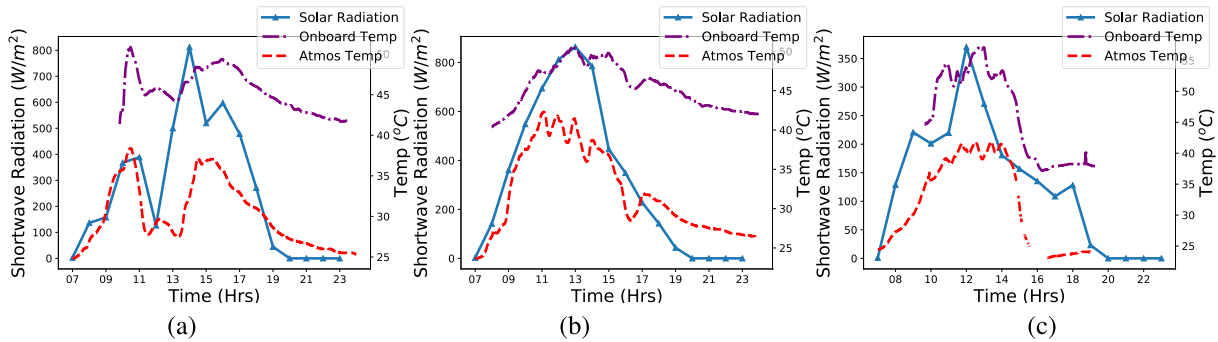


FIGURE 3. Solar radiation versus onboard and atmospheric temperature (a) 29th Oct. (b) 30th Oct. (c) 31st Oct.

TABLE 1. System parameters.

Parameters	Values/Settings
Transmission	uplink
Acknowledgment	Yes
Activation method	OTAA
Code rate	4/5
GW transmit power	27 dBm
Spreading factor	10
Bandwidth	125 kHz
Packet Size	21 bytes
End-device output power	+14 dBm
End-device Antenna gain	+5 dBi
Carrier Frequency	923 MHz

using a duty-cycle that limits the amount of time a device is allowed to transmit from 0.1% (3.6 s per hour) up to 10% (360 s per hour) [15]. Due to the restriction of the LoRaWAN duty-cycle, the experiment was observed for only three consecutive days (morning to late evening) from 29th till 31st of October 2020.

III. EXPERIMENTS AND Results

In this section, the effect of solar radiation, temperature, humidity, and rain are presented. The correlation of the weather parameters and the RSSI of the LoRa are analyzed and the computation of the Pearson correlation coefficient were used to measure the degree of the linear dependence between the solar radiation and RSSI, and between the temperature and the RSSI.

A. EFFECT OF SOLAR RADIATION AND TEMPERATURE

The solar radiation values obtained from the Meteoblue online weather station for the location Skudai [16] were plotted against the onboard and atmospheric temperatures as shown in Figs. 3 (a), (b), and (c) for the three experimental days. The energy radiated by the sun is known as solar energy and it consists of the visible part known as shortwave radiation measured in W/m^2 . It can be seen that solar radiation has quite a significant effect on the atmospheric and onboard temperature where a positive trend can be observed.

From Fig. 3 it can be shown that as the atmospheric temperature increases, the onboard temperature of the LoRa

radio increases. The increase of the onboard temperature is a result of the increase in the junction temperature T_j of the semiconductors such as the microprocessor and LoRa radio. It is a function of the ambient temperature T_a , the dissipated power P_d , and the thermal resistance R_{ja} , where $T_j = T_a + (P_d \times R_{ja})$ [17]. This implies that the atmospheric weather has a direct impact on the onboard LoRa radio.

The impact of the solar radiation and the temperature on the LoRa RSSI is shown in Fig. 4 (a), (b), and (c). From the visual inspection of Figs. 4 (a), (b), and (c), a positive correlation of the solar radiation with the RSSI for the three different days is observed. It can be shown that higher RSSI values were observed during the high solar radiation period compared to periods with low solar radiation. For instance, in Fig 4 (a) and (b) on the 29th and 30th October, high values of solar radiation with peak values of about $800 W/m^2$ were observed during the daytime and within this period, stronger RSSI values were observed. On the 31st, lower values of solar radiation were observed compared to the 29th and 30th. This could be due to the absorption, scattering, or reflection by air molecules, water vapor, and cloud on the rainy day. However, high solar radiation from 8.00 am until about 3:00 pm was observed with a corresponding increase in the onboard temperature and atmospheric temperature as well as the RSSI. The degradation in the RSSI values during low solar radiations can lead to a loss in packet delivery especially for nodes that are located at the edge of the cell.

Further analysis of Fig. 4 (a), (b), and (c) show that stronger RSSI signals are obtainable when the onboard temperature is within the range of 40 - 50 °C and the atmospheric temperature is within the range of 30 - 40 °C. The same pattern can be observed on the 30th and 31st of October 2020, in Fig. 4 (b) and (c) respectively. The result shows that temperature has an impact on the RSSI of the LoRa link as reported in previous studies [7], [8], [11].

The periodic pattern of RSSI obtained during the three days and the positive correlation to the solar radiation observed can be attributed to the effect of the refractive index of the troposphere as suggested in [12]. Other factors that may have influenced this can be attributed to the effect of evaporation duct on radio propagation at very high frequency (30-300 MHz)

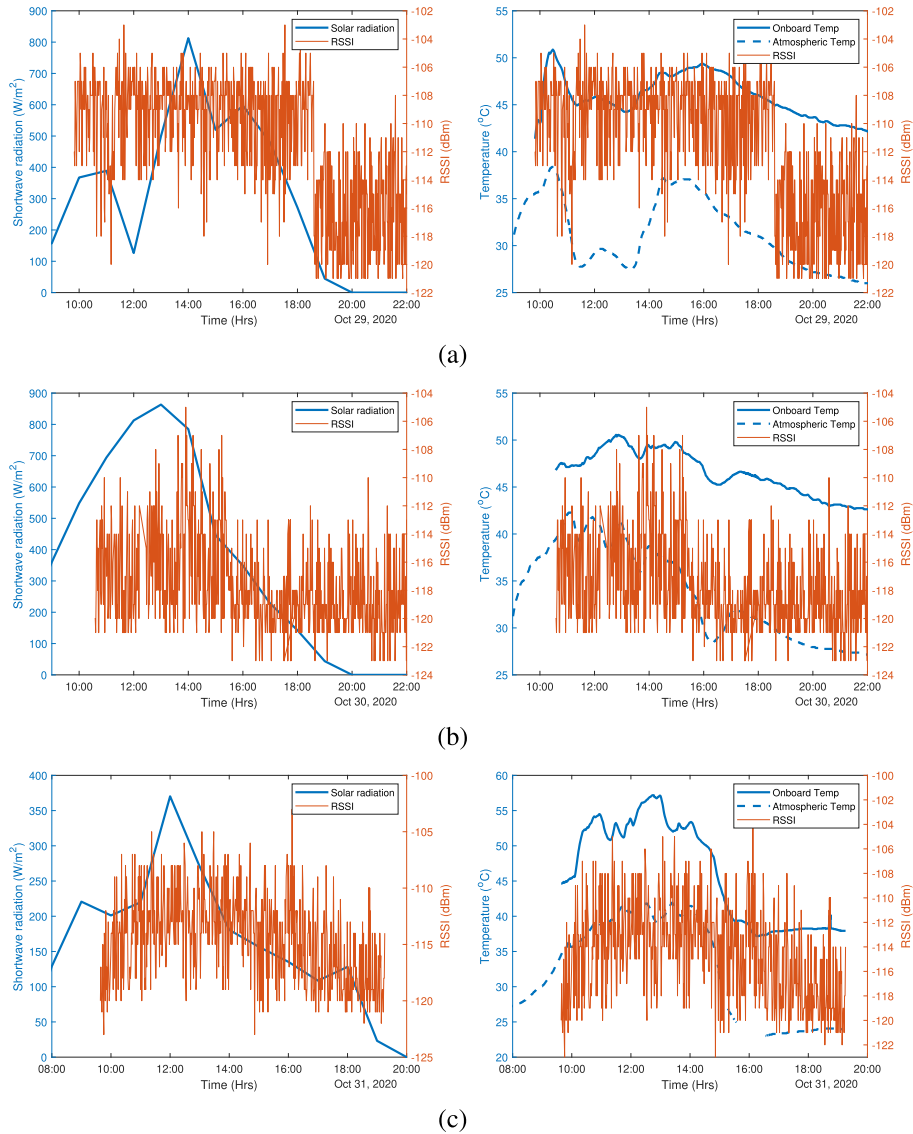


FIGURE 4. RSSI variations with solar radiation and temperature (a) 29th Oct. clear sky, (b) 30th Oct. clear sky and (c) 31st Oct. clear sky condition in the morning and rainy condition in the afternoon.

and ultra-high frequency (300-3000 MHz) especially in tropical climates discussed in [18]. The evaporation duct is a function of the difference in the sea and air temperature which can lead to enhanced signal propagation. There is a need for further research on how the atmospheric condition influences the LoRa link propagation in order to get a better insight.

Further analysis on the correlation of RSSI with the solar radiation can be determined using the covariance and the Pearson’s correlation expressed as follows [19]

$$cov(D1, D2) = \frac{(\sum(D1 - \mu(D1)) \times D2 - \mu(D2))}{(n - 1)} \quad (1)$$

$$\rho_{D1,D2} = \frac{cov(D1, D2)}{std(D1) \times std(D2)} \quad (2)$$

where μ , std and cov are the mean, standard deviation, and covariance, respectively. The $D1$ present the RSSI while $D2$ represent the solar radiation or temperature vectors.

The hourly mean values of the RSSI were correlated using (1) and (2) with the atmospheric temperature obtained from the Hobo rain gauge and the solar radiation and the results are summarized in Table 2 and 3, respectively. The hourly mean values of the RSSI \overline{RSSI}_{1h} were computed as:

$$\overline{RSSI}_{1h} = \frac{1}{n} \sum RSSI_{1h} \quad (3)$$

where n is the total number of RSSI values obtained in duration of one hour and the $RSSI_{1h}$ is the RSSI values received within the LoRa eight channels in the frequency band for one hour. The use of the average value helps to exploit frequency diversity which mitigates the fading effects when analyzing weather conditions [20].

An example of the scatter plot and linear regression of the RSSI variation with the solar radiation, onboard temperature, and atmospheric temperature for one of the days is shown in Figs 5 (a), (b) and (c), respectively. It can be seen that

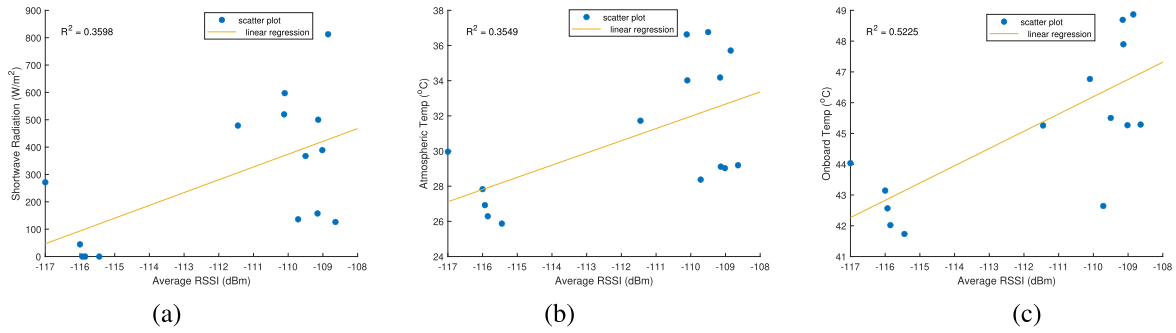


FIGURE 5. Scatter plot of RSSI variation in 29th Oct versus (a) Solar radiation (b) Atmospheric temperature (c) Onboard temperature.

TABLE 2. Correlation Test: solar radiation Vs atmospheric temperature.

Days	Covariance	Pearson's correlation
29th October	651.73	0.701
30th October	1613.80	0.934
31st October	535.46	0.784

TABLE 3. Correlation test: Solar radiation Vs RSSI.

Days	Covariance	Pearson's correlation
29th October	492.55	0.600
30th October	314.92	0.804
31st October	137.24	0.690

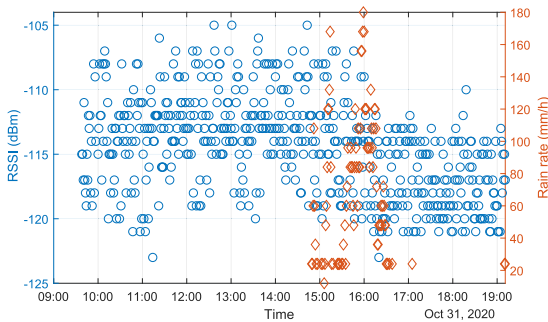


FIGURE 6. RSSI variation with rain intensity during clear sky and rain period.

the low values of RSSI are available at low values of solar radiation and onboard and atmospheric temperature, respectively. The Pearson's correlation test of the solar radiation with the RSSI and the atmospheric temperature are presented in Table 2 and 3.

From Table 2 and 3, Pearson's correlation values are positive, which indicates a positive correlation in the solar radiation and atmospheric temperature, and solar radiation and RSSI for the days observed, respectively.

B. EFFECT OF RAIN

Rain attenuation is one of the factors that affect radio propagation, especially in the tropical and equatorial regions due to the high level of precipitation [21]–[23]. Heavy and regular showers of local convective rain characterize the rainfall process in Malaysia [24] and it is linked to the differen-

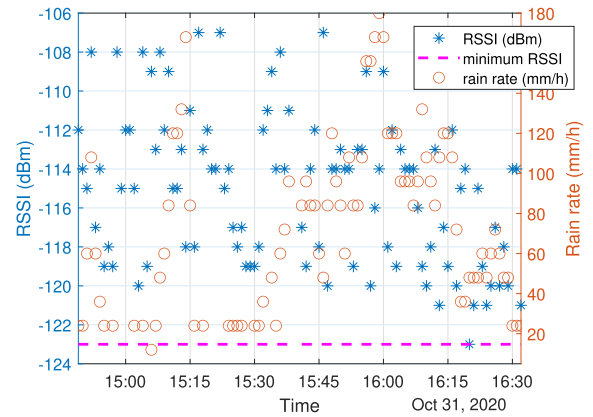


FIGURE 7. RSSI variation with rain intensity during rain period.

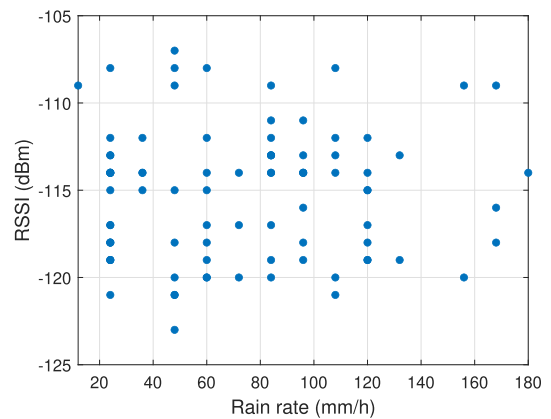
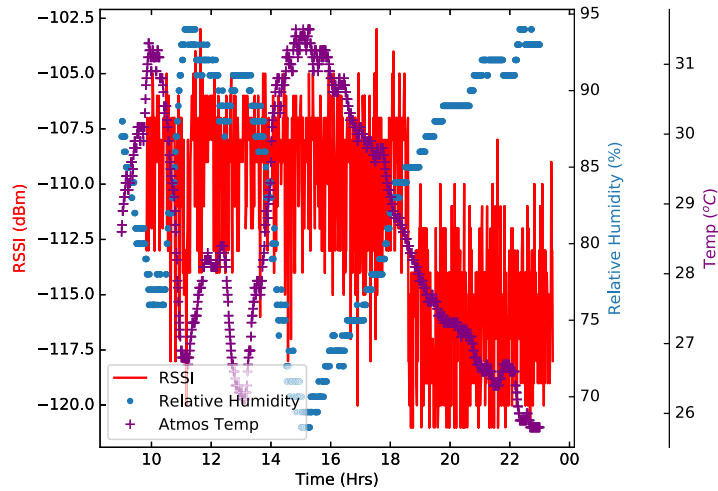
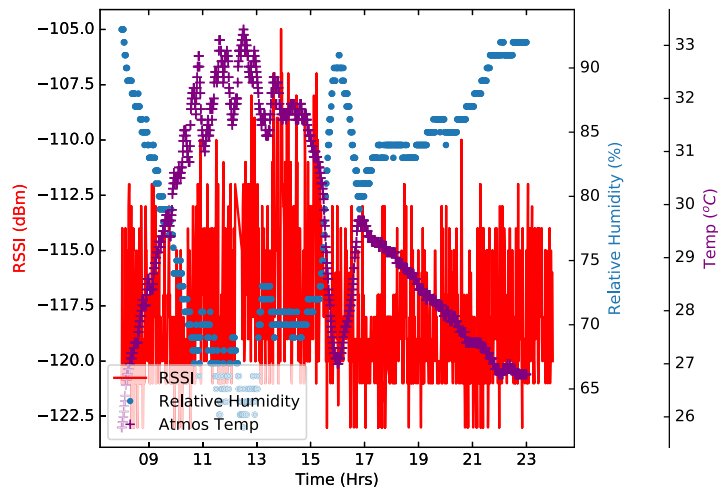


FIGURE 8. RSSI variation with rain intensity.

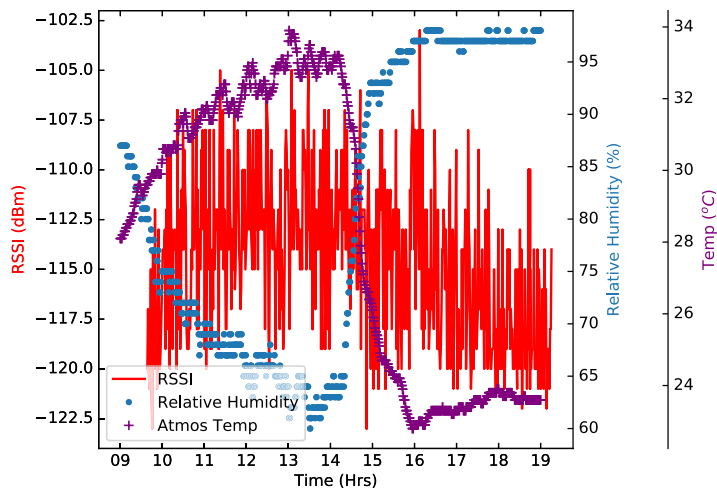
tial heating and cooling of the earth's surface, which varies throughout the day [24]. The rain attenuation is a function of frequency, path-averaged rainfall rate and it depends on temperature and raindrop size distribution (DSD) [24]. The rain attenuation can be expressed as aR_p^b and where R_p is the rain rate with a given period p while a and b are depending on the radio wave frequency and the rain temperature [23]. The DSD results in scattering and attenuation of the electromagnetic wave [25] and is known to be the dominant parameter that causes signal degradation that leads to propagation attenuation especially for frequencies above 10 GHz



(a)



(b)



(c)

FIGURE 9. RSSI variation with relative humidity (a) 29th Oct., (b) 30th Oct., and (c) 31st Oct.

[22], [24]. The DSD for tropical regions like Malaysia and Singapore varies between 1 mm and 6 mm [22], [24], [26]. The transmission frequency of LoRa is 923 MHz, with a wavelength of 0.32 m which is far greater than the DSD values. Hence, the rain is expected to have less impact on the LoRa RSSI performance. To verify the impact of the rain, the RSSI was observed during the rainfall period on the 31st of October from 3.00 pm to 5.00 pm. The rain rate was measured using HOBO data logging rain gauges installed in the link paths. The data logging rain gauge system is battery-powered and includes a data logger with a tipping bucket rain gauge of 0.2 mm sensitivity. The rain gauges record the rainfall that occurs every minute, i.e., at an integral multiple of 12 mm/h where the unit of rain rate is in millimeters per hour (mm/h) [23].

The rainfall rates vary from 12 mm/h to 180 mm/h as shown in Fig. 6. It can be shown that the trend of RSSI from around 9:30 am till around 4:30 pm is almost the same, while the RSSI degradation after 4:30 pm follows the same trend of degradation till 7:00 pm. This indicates that the rain has no significant effect on the degradation of the RSSI along the path of the LoRa link of around 916.26 m. The down-pour of rain resulted in a drop in the solar radiation which consequently reduces the RSSI of the LoRa link. However, there was no significant impact on the RSSI, and all packets sent during the rain were delivered successfully. This can be attributed to the fact that the DSD is very small compared to the wavelength of the LoRa transmission frequency (sub-1 GHz) and also because the CSS modulation of LoRa is robust against multipath effects.

The variation of RSSI during the rain period is shown in Fig. 7. In Fig. 7 the left side of the y-axis represents the RSSI while the right side represents the rain rate values and the pink dash line represents the minimum acquired value of RSSI during the clear sky conditions. It can be shown that during the rain period, no value of RSSI below -123 dBm; implying that the rain attenuation is 0 dB. Moreover, we can get the maximum value of RSSI of -107 dBm during this period of rain. To further clarify this point, Fig. 8 shows the RSSI versus rain rate; the RSSI is in the range between -107 to -123 dBm for the value of the rain rate of 48 mm/h, which is the same variation during the clear sky condition (no rain). Moreover, at a high rain rate of 180 mm/h, the RSSI value of -115 dBm outperforms about 8 dB above the lowest value of RSSI.

C. EFFECT OF HUMIDITY

Further studies were carried out to ascertain the effect of humidity on the RSSI signal. The amount of water vapor in the air is measured by humidity. The amount of water vapor (absolute humidity) in the air compared to the maximum amount of water vapor (saturated humidity) at the same temperature and pressure is described as relative humidity and it is measured in percentage (%). The humidity data were obtained from the automatic weather station (Davis 6152 wireless vantage Pro2 weather station) installed in the

Wireless Communication Center, UTM Johor Campus. The impact of relative humidity on the RSSI can be observed in Fig. 9 (a), (b), and (c). In Fig 9 (a), (b), and (c) the values of RSSI do not vary according to the values of relative humidity. Hence, there is no positive correlation that can be observed. The lack of correlation between the relative humidity and RSSI signal is in agreement with the report of the study in [12].

IV. CONCLUSION

In this paper, the diurnal variation and the effects of the weather conditions based on the LoRa link in a LoRaWAN setup was presented. The analyses of the impact of onboard temperature, atmospheric temperature, relative humidity, and solar radiation on the LoRa communication link were provided. The effect of rain conditions on the LoRa link was also reported. The RSSI measurement for three consecutive days showed similar patterns with stronger signals during the day when the solar radiation is high. A positive correlation between solar radiation and RSSI was observed. This could be due to the influence of the activity of the troposphere such as refractive index, evaporation ducts, and other meteorological conditions that were prevalent. Further research is needed to investigate the effect of meteorological conditions such as positive air-sea temperature, the existence of high-pressure centers, refractivity of the lower troposphere.

The increase in solar radiation also increases the onboard and atmospheric temperature which can be caused by the junction temperature of the semiconductor of the LoRa device. The precipitation almost has no impact on the RSSI in the LoRa system even at a high rainfall rate of 180 mm/h from this study at the propagation distance of 916.25 m and the level of the RSSI observed. This characteristic observed shows the need for further studies on the effect of weather conditions on LoRa. Findings from this study will be useful in the propagation modeling of LoRa (including other closely related IoT transceivers) and the reliability studies of LoRa application in IoT use cases. Future work will examine the effect of prevailing meteorological conditions on the RSSI for multiple links (more nodes), different transmit power, and different LoRa physical settings.

ACKNOWLEDGMENT

The authors would like to acknowledge the funding and support from the 5G and Beyond Wireless Innovation Center, Technology Park, King Mongkut's University of Technology North Bangkok, Thailand.

REFERENCES

- [1] O. Elijah, T. A. Rahman, I. Orikumhi, C. Y. Leow, and M. H. D. N. Hindia, "An overview of Internet of Things (IoT) and data analytics in agriculture: Benefits and challenges," *IEEE Internet Things J.*, vol. 5, no. 5, pp. 3758–3773, Oct. 2018.
- [2] O. Hahm, E. Baccelli, H. Petersen, and N. Tsiftes, "Operating systems for low-end devices in the Internet of Things: A survey," *IEEE Internet Things J.*, vol. 3, no. 5, pp. 720–734, Oct. 2016.
- [3] R. Fernandes, R. Oliveira, M. Luis, and S. Sargento, "On the real capacity of LoRa networks: The impact of non-destructive communications," *IEEE Commun. Lett.*, vol. 23, no. 12, pp. 2437–2441, Dec. 2019.

- [4] T. Elshabrawy and J. Robert, "Closed-form approximation of LoRa modulation BER performance," *IEEE Commun. Lett.*, vol. 22, no. 9, pp. 1778–1781, Sep. 2018.
- [5] M. Sidorov, P. V. Nhut, Y. Matsumoto, and R. Ohmura, "LoRa-based precision wireless structural health monitoring system for bolted joints in a smart city environment," *IEEE Access*, vol. 7, pp. 179235–179251, 2019.
- [6] T. J. Sheng, M. S. Islam, N. Misran, M. H. Baharuddin, H. Arshad, M. R. Islam, M. E. H. Chowdhury, H. Rmili, and M. T. Islam, "An Internet of Things based smart waste management system using LoRa and tensorflow deep learning model," *IEEE Access*, vol. 8, pp. 148793–148811, 2020.
- [7] C. A. Boano, M. Cattani, and K. Römer, "Impact of temperature variations on the reliability of lora," in *SENSORNETS*, 2018, pp. 39–50.
- [8] M. Cattani, C. Boano, and K. Römer, "An experimental evaluation of the reliability of LoRa long-range low-power wireless communication," *J. Sensor Actuator Netw.*, vol. 6, no. 2, p. 7, Jun. 2017.
- [9] C. A. Boano, M. Zuniga, J. Brown, U. Roedig, C. Keppityagama, and K. Romer, "TempLab: A testbed infrastructure to study the impact of temperature on wireless sensor networks," in *Proc. IPSN-14 Proc. 13th Int. Symp. Inf. Process. Sensor Netw.*, Apr. 2014, pp. 95–106.
- [10] N. Souza Bezerra, C. Åhlund, S. Saguna, and V. A. de Sousa, "Temperature impact in LoRaWAN—A case study in Northern Sweden," *Sensors*, vol. 19, no. 20, p. 4414, 2019.
- [11] N. Jetic, M. Simic, and Z. Stamenkovic, "Impact of environmental parameters on SNR and RSS in LoRaWAN," in *Proc. Int. Conf. Electr., Commun., Comput. Eng. (ICECCE)*, Jun. 2020, pp. 1–6.
- [12] T. Ameloot, P. Van Torre, and H. Rogier, "Periodic LoRa signal fluctuations in urban and suburban environments," in *Proc. 13th Eur. Conf. Antennas Propag. (EuCAP)*, Mar./Apr. 2019, pp. 1–5.
- [13] *Loriot*. Accessed: Apr. 1, 2019. [Online]. Available: <https://www.loriot.io/>
- [14] *H. R. Data Logging Rain Gauge*. Accessed: Sep. 4, 2020. [Online]. Available: <https://www.onsetcomp.com/files/data-sheet/Onset%20HOBO%20RG3%20Rain%20Gauge.pdf>
- [15] M. Saelens, J. Hoebeke, A. Shahid, and E. D. Poorter, "Impact of EU duty cycle and transmission power limitations for sub-GHz LPWAN SRDs: An overview and future challenges," *EURASIP J. Wireless Commun. Netw.*, vol. 2019, no. 1, pp. 1–32, Dec. 2019.
- [16] *Meteoblue*. Oct. 2020. [Online]. Available: https://www.meteoblue.com/en/weather/week/skudai_malaysia_1732745
- [17] J. Forster and C. Lopez, "Junction temperature during burn-in: How variable is it and how can we control it?" in *Proc. 23rd Annu. IEEE Semiconductor Thermal Meas. Manage. Symp.*, Mar. 2007, pp. 168–173.
- [18] S. D. Gunashekar, D. R. Siddle, and E. M. Warrington, "Transhorizon radiowave propagation due to evaporation ducting," *Resonance*, vol. 11, no. 1, pp. 51–62, Jan. 2006.
- [19] H. Zhou, Z. Deng, Y. Xia, and M. Fu, "A new sampling method in particle filter based on pearson correlation coefficient," *Neurocomputing*, vol. 216, pp. 208–215, Dec. 2016.
- [20] J. Luomala and I. Hakala, "Effects of temperature and humidity on radio signal strength in outdoor wireless sensor networks," in *Proc. Federated Conf. Comput. Sci. Inf. Syst.*, Oct. 2015, pp. 1247–1255.
- [21] A. M. Al-Saman, M. Cheffena, M. Mohamed, M. H. Azmi, and Y. Ai, "Statistical analysis of rain at millimeter waves in tropical area," *IEEE Access*, vol. 8, pp. 51044–51061, 2020.
- [22] L. S. Kumar, Y. Hui Lee, and J. Teong Ong, "Truncated gamma drop size distribution models for rain attenuation in singapore," *IEEE Trans. Antennas Propag.*, vol. 58, no. 4, pp. 1325–1335, Apr. 2010.
- [23] S.-H. Fang, Y.-C. Cheng, and Y.-R. Chien, "Exploiting sensed radio strength and precipitation for improved distance estimation," *IEEE Sensors J.*, vol. 18, no. 16, pp. 6863–6873, Aug. 2018.
- [24] H. Y. Lam, L. Luini, J. Din, C. Capsoni, and A. D. Panagopoulos, "Investigation of rain attenuation in equatorial kuala lumpur," *IEEE Antennas Wireless Propag. Lett.*, vol. 11, pp. 1002–1005, 2012.
- [25] M. Marzuki, T. Kozu, T. Shimomai, W. L. Randeu, H. Hashiguchi, and Y. Shibagaki, "Diurnal variation of rain attenuation obtained from measurement of raindrop size distribution in equatorial indonesia," *IEEE Trans. Antennas Propag.*, vol. 57, no. 4, pp. 1191–1196, Apr. 2009.
- [26] H. Y. Lam, J. Din, and S. L. Jong, "Statistical and physical descriptions of raindrop size distributions in equatorial Malaysia from disdrometer observations," *Adv. Meteorol.*, vol. 2015, Apr. 2015, Art. no. 253730.



OLAKUNLE ELIJAH (Member, IEEE) received the B.Eng. degree from the Federal University of Technology Minna, Minna, Nigeria, in 2003, the M.Sc. degree in micro-electronics and computing from Bournemouth University, Poole, U.K., in 2008, the master's degree in advance micro-electronics from Bolton University, Bolton, U.K., in 2010, and the Ph.D. degree from the Universiti Teknologi Malaysia, Johor Bahru, Malaysia, in 2018. He was a Field Engineer with Kuyet Nigeria Ltd., Lagos, Nigeria, in 2006. From 2011 to 2013, he was the MD/CEO with Mircoscale Embedded Limited, Abuja, Nigeria. He is currently conducting research in the field of wireless communications and the IoT as a Postdoctoral Fellow with the Wireless Communication Centre, Higher Institution Centre of Excellence (HiCoE) Malaysia. His current research interests include embedded systems, wireless communications, massive MIMO, interference mitigation, heterogeneous networks, the IoT with data analysis, and 5G.



SHARUL KAMAL ABDUL RAHIM (Senior Member, IEEE) received the degree in electrical engineering from the University of Tennessee, USA, in 1996, the M.Sc. degree in engineering (communication engineering) from the Universiti Teknologi Malaysia (UTM), Skudai, in 2001, and the Ph.D. degree in wireless communication system from the University of Birmingham, U.K., in 2007. He is currently a Professor with the Wireless Communication Centre, Faculty of Electrical Engineering, UTM. He has published over 50 journal articles and technical proceedings on rain attenuation, smart antenna systems, microwave design, and reconfigurable antenna in national and international journals and conferences. His research interest includes smart antenna on communication systems. He is a member of the IEEE Malaysia Section, a member of the Board of Engineer Malaysia, and a member of the Institute of Engineer Malaysia and the Eta Kappa Nu Chapter (International Electrical Engineering Honour Society, University of Tennessee).



VITAWAT SITTAKUL received the B.Eng. degree in telecommunication from Chulalongkorn University, Bangkok, Thailand, in 2000, the M.Sc. degree (Hons.) in optical and communication systems from Northumbria University, Newcastle, U.K., in 2003, and the Ph.D. degree from the Department of Electrical and Electronic Engineering, University of Bristol, Bristol, U.K., in 2006. From 2003 to 2004, he was a Measurement Engineer with Fabinet, where he was a global engineering and manufacturing services provider. From 2004 to 2006, he was a Senior RF Engineer with Advance Information Service Company, Ltd. (AIS), which is the biggest mobile service provider in Bangkok. From 2006 to 2009, he was a Research Assistant with the University of Bristol. From 2009 to 2015, he worked as an RF Metrologist with the National Institute of Metrology, Thailand. He is currently an Associate Professor with the Department of Electrical and Electronics Engineering Technology and the Head of the 5G and Beyond Wireless Innovation Center, King Mongkut's University of Technology North Bangkok, Thailand.



AHMED M. AL-SAMMAN received the B.S. degree in electrical-electronics and telecommunications engineering from IBB University, Yemen, in 2004, and the M.Eng. and Ph.D. degrees in electrical-electronics and telecommunications engineering from the Universiti Teknologi Malaysia (UTM), Malaysia, in 2013 and 2017, respectively. From 2004 to 2010, he was an Engineer with the Department of Management of Frequency Spectrum, Ministry of Communications and Information Technology, Yemen. From July 2017 to July 2019, he held a postdoctoral position with the Innovation Centre for 5G (IC5G), UTM. He is conducting postdoctoral research with the Faculty of Engineering, Norwegian University of Science and Technology (NTNU). His research interests include signal processing, channel propagation, UWB systems, and millimeter wave communication for 5G and 6G systems.



JAFRI BIN DIN received the B.Sc. degree in electrical engineering from Tri-State University, Angola, IN, USA, in 1988, and the Ph.D. degree from the Universiti Teknologi Malaysia (UTM), Johor, Malaysia, in 1997. From 2008 to 2015, he was the Head of Departments, Undergraduate Academic Manager, and the Deputy Dean (Development) of the Faculty of Electrical Engineering (FKE), UTM. He is currently the Director of the Wireless Communication Centre, UTM. His research activities have been correlated to the fields of radio wave propagation, satellite propagation, high-altitude platform station (HAPS), satellite TV broadcasting, weather radar, and sound techniques for fisheries industry.



MICHAEL CHEFFENA received the M.Sc. degree in electronics and computer technology from the University of Oslo, Oslo, Norway, in 2005, and the Ph.D. degree in telecommunications from the Norwegian University of Science and Technology (NTNU), Trondheim, Norway, in 2008. He was a Visiting Researcher with the Communications Research Center, Ottawa, ON, Canada, in 2007. From 2009 to 2010, he conducted his postdoctoral study at the University Graduate Center, Kjeller, Norway, and the French Space Agency, Toulouse, France. He is currently a Full Professor with NTNU. His current research interests include the modeling and prediction of radio channels for both terrestrial and satellite links.



ABDUL RAHMAN THAREK received the B.Sc. degree (Hons.) in electrical engineering from the University of Strathclyde, Glasgow, U.K., the M.Sc. degree in communication engineering from the University of Manchester Institute of Science and Technology (UMIST), Manchester, U.K., and the Ph.D. degree in mobile communication from the University of Bristol, Bristol, U.K. He is currently a Professor of wireless communication with the Faculty of Electrical Engineering, Universiti Teknologi Malaysia, Johor Bahru, Malaysia. He is the Director of the Wireless Communication Centre (WCC), Faculty of Electrical Engineering, Universiti Teknologi Malaysia, and also conducting research related to mobile communications, antenna and propagation. Since 1988, he has been conducting various short courses related to mobile and satellite communication to the telecommunication industry and government agencies. He has authored more than 300 scientific articles in journals and conferences. He is also a consultant for many communication companies and an active member in several research academic entities. He received many national and international awards.

• • •